Environmental Pollution 254 (2019) 112974

Contents lists available at ScienceDirect

Environmental Pollution

journal homepage: www.elsevier.com/locate/envpol

Moss facilitating mercury, lead and cadmium enhanced accumulation in organic soils over glacial erratic at Mt. Gongga, China☆

Xun Wang [a, b], Wei Yuan [b], Xinbin Feng [b, *], Dingyong Wang [a], Ji Luo [c]

[a] College of Resources and Environment, Southwest University, Chongqing, 400715, China
[b] State Key Laboratory of Environmental Geochemistry, Institute of Geochemistry, Chinese Academy of Sciences, Guiyang, 550081, China
[c] Key Laboratory of Mountain Surface Processes and Ecological Regulation, Institute of Mountain Hazards and Environment, Chinese Academy of Sciences & Ministry of Water Conservancy, Chengdu, 610041, China

ARTICLE INFO

Article history:
Received 24 June 2019
Received in revised form
26 July 2019
Accepted 26 July 2019
Available online 27 July 2019

Keywords:
Glacier retreat
Heavy metal accumulation
Moss uptake
Mercury isotopes

ABSTRACT

Moss is usually as an initial colonizer in alpine glacier retreated regions. We hypothesized that moss can significantly facilitate the toxic metals accumulation in alpine ecosystems based on its strong ability of absorption and the role in soil development. Hence, we investigated the trace element pool sizes and enrichment factors, especially for mercury (Hg) by using the Hg isotopic compositions to determine the source contributions in a moss-dominated ecosystem over glacial erratic in Eastern Tibetan Plateau. Results show that Hg, lead (Pb) and cadmium (Cd) are highly enriched in organic soils. Specifically, Cd concentration is 5–20 times higher than the safety limit of the acid soil (pH $\leq$ 5.5) in China. Atmospheric depositions dominantly contribute to the Pb and Cd sources in organic soils, and followed by the moraine particles influences. The lowering pH in organic soils increasing with glacial retreated time results in the desorption of Cd in organic soils. Atmospheric Hg^0 uptake by moss predominantly contributes to the Hg sources in organic soils. The average Pb accumulation rate over last 125-year is about 5.6 ± 1.0 mg m^{-2} yr^{-1}, and for Cd is 0.4 ± 0.1 mg m^{-2} yr^{-1}, and for Hg^0 is 27.6 ± 3.2 μg m^{-2} yr^{-1}. These elevated accumulation rates are caused by the high moss biomass and elevated atmospheric Hg, Pb and Cd pollution levels in China and neighbouring regions. Our study indicates that the moss not only as the bioindicator, but also plays an important role in the hazardous metal biogeochemical cycling in alpine regions.

1. Introduction

Alpine areas are very sensitive to global warming and human activities. Of major significances are the alpine glaciers (Dyurgerov, 2003; Dyurgerov and Meier, 1997), which have been shrinking rapidly due to the accelerated warming in recent decades (Brun et al., 2017; Yao et al., 2012). As glaciers retreat, glacial erratic and moraine (i.e., glacial debris, such as regolith and rock flour) tend to establish an entirely new ecosystem (e.g., forest, steppe, and tundra). Meanwhile, substantial hazardous metals through atmospheric depositions are introduced into this new ecosystem, leading to their concentrations largely increase compared to previously existed only in much smaller quantities (Bing et al., 2016; Bing et al., 2014). The enhanced accumulation of these toxic metals in alpine ecosystems poses a distinct pollution risk.

Moss is usually as an initial colonizer in glacial retreated regions, and plays an important role in the soil development (Cannone and Gerdol, 2003; Favero-Longo et al., 2012; Frenot et al., 1998; Raffl et al., 2006). Specifically, moss is as the most widely used bioindicator to monitor the toxic metal pollution levels because of its cost-effectiveness, diversity of habitats, structural simplicity, rapid multiplication rate and easier sampling (Stankovic et al., 2018; Tyler, 1990). Recent studies have revealed that moss has a significant contribution to the nutrient element biogeochemical cycling in terrestrial ecosystems (Elbert et al., 2012; Nakatsubo et al., 2015). For example, ~50% of biological nitrogen fixing in terrestrial ecosystems is caused by moss and lichen (Elbert et al., 2012). High levels of rainfall and frequent cloud cover commonly occur in alpine regions, thus inducing intensive coverage of moss in alpine ecosystems (Britton et al., 2018; Miguez et al., 2017). Compared to earlier studies that highlighted the moss biomonitoring of atmospheric toxic metal pollution levels (Stankovic et al., 2018; Tyler, 1990), we hypothesized moss can significantly facilitate the toxic

☆ This paper has been recommended for acceptance by Jörg Rinklebe

* Corresponding author.
E-mail address: fengxinbin@vip.skleg.cn (X. Feng).

https://doi.org/10.1016/j.envpol.2019.112974
0269-7491/

metals accumulation in alpine ecosystems based on its high biomass and strong ability of absorption to these toxic metals.

One of essential issues is to understand the toxic metal sources and accumulation pathways in alpine regions. The cold trapping, which is associated with the intensive precipitation and cloud water in alpine regions, is highlighted to result in the elevated toxic metal depositions (Bacardit and Camarero, 2010; Bing et al., 2016). Most of toxic metals (except for mercury) emitted to the atmosphere as fine particulates subject to atmospheric transport over days to weeks of residence time before deposited onto the Earth's surface including vegetation (Tchounwou et al., 2012; Tóth et al., 2016). Different from most of toxic metals whose transport and deposition are highly related to the particle form, elemental mercury (Hg^0) vapor plays an important role in biogeochemical cycling of Hg in the environment (Lindberg et al., 2007; Obrist et al., 2018). Mercury in terrestrial ecosystems is primarily from three origins: deposition of atmospheric Hg^0 (e.g., via litterfall), deposition of atmospheric Hg^{II} (e.g., via precipitation), and geogenic sources (e.g., weathering of rocks), yet their relative importance in alpine ecosystems remains poorly studied (Lindberg et al., 2007; Obrist et al., 2018). For example, Zhang et al. (2013) reported atmospheric Hg depositions increased with the elevation at a forest site of Southwest China and suggested the important influences from cold trapping; while such elevation associated trend was insignificant in forests of Eastern Tibet Plateau and soil Hg accumulation was mainly determined by litterfall Hg depositions (Wang et al., 2017).

To determine toxic metal sources, stable isotope techniques have been shown to provide a new mechanistic insight. An earlier research in our study region (Mt. Gongga) used lead (Pb) isotopic ratios to reveal Pb-ore-involved industries and coal combustion mainly dominating the Pb sources in moss and organic soils (Bing et al., 2014). In this study, we further used Hg isotopic compositions to assess the Hg sources. Mercury isotopes undergo mass-dependent fractionation (MDF, reported as δ^{202}Hg) and mass-independent fractionation (MIF, reported as Δ^{199}Hg, Δ^{200}Hg and Δ^{201}Hg) (Blum et al., 2014; Sonke, 2011). Atmospheric Hg^{II} and Hg^0 depositions, and geological Hg sources all show distinctly different Hg isotopic compositions, especially in their MIF signatures (Biswas et al., 2008; Demers et al., 2013; Enrico et al., 2016; Jiskra et al., 2015; Wang et al., 2017; Zheng et al., 2016). Hence, Hg isotopes serve as useful tracers to identify specific sources in alpine regions.

Compared to the conventional forest ecosystems including tall tree, shrub, herb, moss, lichen, and soil profiles, we selected a moss-dominated ecosystem over glacial erratic based on several reasons. One is the simplicity of this moss-dominated ecosystem since without distinct impacts from tall tree species, and soils mainly derived from the decomposition of moss debris. In addition, this ecosystem received much smaller litterfall and throughfall inputs from forest canopy than the forest floor due to the distinct canopy gap over glacial erratic. Moreover, without a root system of moss simplifies the relationships of trace element allocation and transport in vegetation and soils. Finally, it is easy to quantify the variations of trace element pool sizes just by harvesting and chemical analysis of the moss and soil underneath over glacial erratic. It is noteworthy that earlier studies at Mt Gongga have reported the elevated cadmium (Cd), Pb and Hg concentrations in forest organic soils, which attributed to the high atmospheric depositions (Bing et al., 2016; Bing et al., 2014; Fu et al., 2010). In this study, we further highlighted an important role of moss in these toxic metals accumulation in glacier retreated region. We investigated the trace elements pool sizes and enrichment factors, especially for Hg by using the Hg isotopic compositions, to determine the specific source contribution in a moss-dominated ecosystem over glacial erratic. In addition, we used the pool size variations over the glacial erratic chronosequence to estimate the average accumulation rate over last 125-year.

2. Methods

2.1. Sites description

The Hailuogou Glacier, located in the eastern TP, is one of the major glacier systems on the east slope of Mt. Gongga (101°30′–102°15′ E, 29°20′–30°20′ N; peak elevation: 7556 m a.s.l., Fig. 1). The glacier retreated area at the elevation of 2900–3000 m has a ~2 km complete primary vegetation chronosequence. The glacier retreat period of 1890–2005 has been documented in detail (Yang et al., 2015a; Zhou et al., 2013). The annual mean temperature at the study site is 4.2 °C and the annual precipitation ranges from 1800 to 2000 mm, and ~80% of total precipitation occurs in May to November (Luo et al., 2017). The site representing the 2005 retreat has small pioneer tree species (height < 3 m) including big leaf poplar (*Populus purdomii Rehd*), common sea buckthorn (*Hippophae rhamnoides Linn*) and willow (*Salix magnifica Hemsl*). At the sites of retreat during 1990-1958, poplar becomes the dominant species and during 1958-1890, poplar is gradually replaced by the Faber's fir (*Abies fabri Craib*) and dragon spruce (*Picea asperata*). The dominant moss genus over glacial erratic is *Brachythecium, Eurhynchium Actinothuidium, Hylocomium, Pleurozium*, and *Rhizomnium* (Sun et al., 2013).

2.2. Moss and soils sample collections

We set up eight sites (glacier retreat time: 1990, 1985, 1980, 1970, 1958, 1945, 1930, and 1890; elevation ranges 2900–3000 m; Fig. 1) over erratic in glacier retreated regions in May of 2016. The organic soil pH is 6.2 ± 0.1 at 1990, 6.6 ± 0.2 at 1980, 6.2 ± 0.1 at 1970, 6.4 ± 0.1 at 1958, 6.1 ± 0.2 at 1945, 4.7 ± 0.3 at 1930, and 4.8 ± 0.1 at 1890 sites, respectively. The glacial erratic with the area of 2–20 m^2 were selected in this study. Three 0.5×0.5 m subplots over glacial erratic at each site were prepared and the moss and soil profiles underneath were collected. The average thickness of the soil horizon (O horizon) was 1–10 cm depth from site of 1990 to 1890. Within the soil horizon, the Oe (partially decomposed moss debris and some litters) was 0–3 cm in thickness in each subplot, with the Oa horizon (well decomposed humus layer) making up the remainder of soil horizon. In addition, we have collected 6 rock and moraine samples. We sampled moss and soil profiles underneath (0–1 cm depth organic soil, 2–3 cm depth organic soil, 4–5 cm depth organic soil, 6–7 cm depth organic soil, and 8–9 cm depth organic soil) over glacial erratic at 1890 site to determine the Hg isotopic compositions.

2.3. Concentration measurements and pool sizes estimating

Soil samples were air dry in the dark in a clean room and then subsequently ground by agate mortar to 200 mesh sieves (74 μm). Moss samples were ground by a separate electric grinder. Weights of all dry samples have been recorded to calculate the biomass and soil density before grinding. Measurements of Hg in moss and soil samples have been described in detail in our previous works (Wang et al., 2016b; Wang et al., 2017). Mercury concentrations of the samples were measured by a DMA80 Hg analyzer. Standard reference materials were measured in every 10 samples, which yielded a recovery of 95–105%. GBW07405 (GSS-5, $Hg = 290 \pm 40$ ng g^{-1}) was utilized as the soil Hg standard, and GBW10020 (GSB-11, $Hg = 150 \pm 25$ ng g^{-1}) as the vegetation Hg standard.

Concentrations of the other trace elements for moss, soil and rock samples were analyzed by Inductively Coupled Plasma Mass Spectrometry (ICP-MS) and we followed the method procedures of

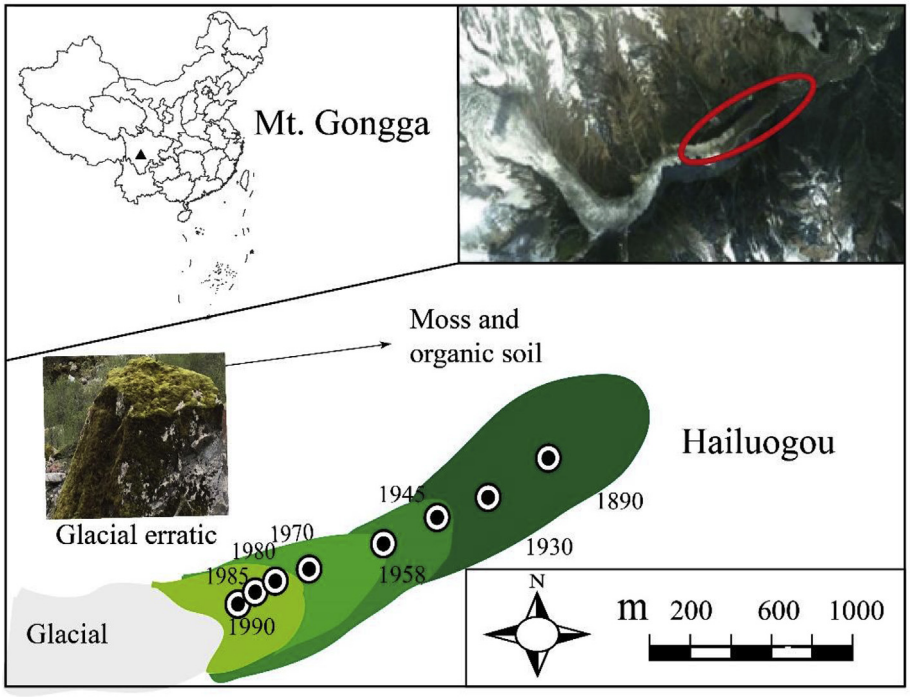

Fig. 1. Sampling sites over a glacial erratic chronosequence at the glacier retreated area of Hailuogou.

USA EPA Method 6020B. Standard reference materials were measured in every 10 samples, which yielded average recoveries of 96–112% (more details in Table S1 of SI, i.e., Support Information) for soil reference materials and 87–106% (more details in Table S2) for vegetation reference materials. Both vegetation and soil reference materials were from the National Quality and Technology Supervision Agency of China (GBW10020 for vegetation reference materials and GBW07405 for soil reference materials). In addition, 3 blank samples in every 50 samples were analyzed to ensure that samples have not been contaminated during the digestion processes. The trace element concentrations in blank samples were all less than 1‰ values of measured samples. Specific trace elements pool sizes were estimated for each site based on the measured concentration in soil and moss, and bulk soil and biomass densities:

$$\text{Pool} = \text{Con}_{\text{moss}} \times \text{Mass\_size}_{\text{moss}} + \sum(\text{Con}_{\text{soils}} \times \text{Mass\_size}_{\text{soils}}) \quad (1)$$

In addition, we used the accumulation factor (AF) and enrichment factor (EF) to assess the degree of accumulation as:

$$\text{AF} = \text{C}_{\text{moss or soils}}/\text{C}_{\text{rock}} \quad (2)$$

$$\text{EF} = (\text{C}/\text{R})_{\text{moss or soils}}/(\text{C}/\text{R})_{\text{rock}} \quad (3)$$

where C is the trace element concentration, and R is the reference element concentration (in this case as Li; reasons can be found in Discussion) in the moss, soil and rock samples. In order to evaluate the degree of trace elements accumulation, the following gradations are proposed (Abrahim and Parker, 2008): AF (or EF) < 1, no/low accumulation; 1 ≤ AF (or EF) < 3, moderate; 3 ≤ AF (or EF) < 6, considerable; 6 ≤ AF (or EF), very high accumulation.

2.4. Stable Hg isotopes measurements and mixing model

The procedure for Hg isotope measurement of moss and soils samples has been described previously (Wang et al., 2017; Wang et al., 2019). Briefly, all samples were processed by a double-stage tube furnace and trapping solutions (anti aqua regia) for Hg preconcentration, and the Hg solutions were diluted to 1 ng mL^{-1} prior to Hg isotope measurement by the Nu-Plasma II MC-ICP-MS. The recoveries of preconcentrating were 95%–103% for the standard reference materials (BCR-482, Moss; GSS-4, Soil) and 93%–103% for all samples. Concentrations and acid matrices of Hg standard solutions (NIST-3133) and UM-Almadén secondary standard solution were matched to the sample solutions. Hg-MDF is reported in δ notation using the unit of permil (‰) referenced to the neighbouring NIST-3133 solution:

$$\delta^{202}\text{Hg}\ (‰) = 1000 \times \left[\left({}^{202}\text{Hg}/{}^{198}\text{Hg}_{\text{sample}}\right)\Big/ \times \left({}^{202}\text{Hg}/{}^{198}\text{Hg}_{\text{NISTSRM3133}}\right) - 1\right] \quad (4)$$

$$\delta^{199}\text{Hg}\ (‰) = 1000 \times \left[\left({}^{199}\text{Hg}/{}^{198}\text{Hg}_{\text{sample}}\right)\Big/ \times \left({}^{199}\text{Hg}/{}^{198}\text{Hg}_{\text{NISTSRM3133}}\right) - 1\right] \quad (5)$$

$$\delta^{200}\text{Hg}\ (‰) = 1000 \times \left[\left({}^{200}\text{Hg}/{}^{198}\text{Hg}_{\text{sample}}\right)\Big/ \times \left({}^{200}\text{Hg}/{}^{198}\text{Hg}_{\text{NISTSRM3133}}\right) - 1\right] \quad (6)$$

$$\delta^{201}\text{Hg}\ (‰) = 1000 \times \left[\left({}^{201}\text{Hg}/{}^{198}\text{Hg}_{\text{sample}}\right)\Big/ \times \left({}^{201}\text{Hg}/{}^{198}\text{Hg}_{\text{NISTSRM3133}}\right) - 1\right] \quad (7)$$

MIF is reported as Δ^{xxx}Hg following the convention suggested by Blum and Bergquist (2007):

$$\Delta^{199}\text{Hg}\ (‰) = \delta^{199}\text{Hg} - 0.2520 \times \delta^{202}\text{Hg} \quad (8)$$

$$\Delta^{200}Hg\ (‰) = \delta^{200}Hg - 0.5024 \times \delta^{202}Hg \quad (9)$$

$$\Delta^{201}Hg\ (‰) = \delta^{201}Hg - 0.7520 \times \delta^{202}Hg \quad (10)$$

UM-Almadén secondary standard solution was analyzed for every 10 samples. To assess if the non-unity recoveries resulting from the double-stage offline combustion-trapping technique induced discernible isotopic bias, we measured BCR 482 and GSS-4 at the beginning of sample pre-concentration sessions. Results of UM-Almadén ($\delta^{202}Hg = -0.54 \pm 0.04‰$, $\Delta^{199}Hg = -0.00 \pm 0.04‰$, $\Delta^{201}Hg = -0.03 \pm 0.02‰$, Mean±1SD, Standard deviation, n = 10) and BCR-482 ($\delta^{202}Hg = -1.67 \pm 0.06‰$, $\Delta^{199}Hg = -0.56 \pm 0.05‰$, $\Delta^{200}Hg = -0.01 \pm 0.03‰$, $\Delta^{201}Hg = -0.58 \pm 0.04‰$, Mean±1SD, n = 6), and GSS-4 ($\delta^{202}Hg = -1.72 \pm 0.08‰$, $\Delta^{199}Hg = -0.34 \pm 0.03‰$, $\Delta^{201}Hg = -0.34 \pm 0.03‰$, $\Delta^{200}Hg = -0.00 \pm 0.02‰$, Mean±1SD, n = 6) are consistent with recommended values (Blum and Bergquist, 2007; Estrade et al., 2010).

The double mixing model using $\Delta^{200}Hg$ signatures was set up to estimate atmospheric Hg^0 and Hg^{II} contributions in moss and soils (details in Discussion)

$$f_1 + f_2 = 1 \quad (11)$$

$$f_1 \times \Delta^{200}Hg_1 + f_2 \times \Delta^{200}Hg_2 = \Delta^{200}Hg_{moss/soil} \quad (12)$$

where f_1 and f_2 are the fraction ratios calculated by $\Delta^{200}Hg$. The uncertainties caused by the bias of $\Delta^{200}Hg$ were considered during the estimate of all fraction ratios. Monte Carlo simulation was applied to generate one million groups of $\Delta^{200}Hg$, which randomly ranging from Mean−SD to Mean + SD. More in detail, the SD for precipitation is 0.14‰, and for atmospheric Hg^0 is 0.04‰, and for samples is 0.04‰. The fraction ratio is estimated as the average of these solutions, which ranges 0–1, during one million times of solving Eq. (10–11).

3. Results

Based on the document of "soil environmental quality risk control standard for soil contamination of agricultural land" (GB 15618-2018) by China government, only the Cd concentration (Table S3) is beyond this control standard, more in detail, 5–20 times greater than the Cd safety standard in acid soil ($pH \leq 5.5$; $0.3\ \mu g\ g^{-1}$), and even 1–4 times greater than the Cd pollution risk limit ($pH \leq 5.5$; $1.5\ \mu g\ g^{-1}$). Fig. 2 demonstrates highest AF for Hg (up to 53, very high accumulation), followed by Cd (cadmium, ~5.8, considerable accumulation) and Pb (~2.6, moderate accumulation), and finally ≤1 for the other trace elements. Hence, it is essential to determine the Hg, Cd and Pb accumulation pathways and sources in this moss-dominated ecosystem.

Fig. 3(1–6) exhibit variations of concentration and pool size for Pb, Cd and Hg. The Hg, Pb and Cd concentrations in moss are generally lower than in Oe and Oa ($p < 0.05$, by T-paired test). The pool size variations in moss, Oe and Oa have been shown in Fig. S1. The pool sizes for Pb, Cd and Hg are all highest in Oa (average values of 51–58%), and in Oe are comparable to in moss. In addition, the fraction of Pb, Cd and Hg pool sizes in moss over total pool size decreases with the age of organic soils. The Hg and Pb concentrations and total pool sizes both exhibit the significant increase from 1990 to 1890 sites ($p < 0.05$). A peak of total pool size occurs for Cd around 1990 and 1958 sites, and for Pb only around 1958 site.

Fig. 4(1–3) depict variations of EF for Pb, Cd and Hg. Overall, the EF values for Hg, Pb and Cd are all greater than 10, and EF values in moss and Oe are higher than in Oa for these toxic metals ($p < 0.05$, by T-paired test). This suggests the enhanced accumulation for Hg, Cd and Pb, consistent with findings in earlier studies (Bing et al., 2016; Bing et al., 2014; Fu et al., 2010). Specifically, Hg in moss and soils is most enhanced (~54 times greater than in moraine), and its EF is up to 45–1048. This suggests a specific biogeochemical cycling of Hg. In addition, the EF values for Hg and Pb both exhibit a significant increase from 1990 to 1890 sites ($p < 0.05$).

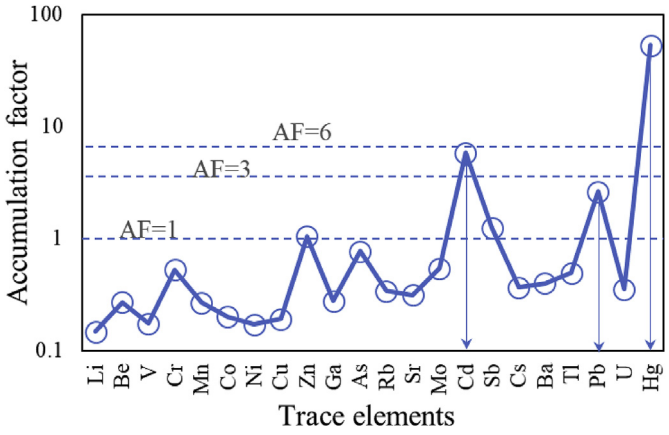

Fig. 2. Average accumulation factors (AF, average concentration in moss and soil over concentration in rock) for all trace elements over the glacial erratic chronosequence.

The Hg isotopic compositions at 1890 site are shown in Fig. 5(1–2). Moss and soils have distinct negative $\delta^{202}Hg$ ranging from −3.17‰ to −1.91‰, and −0.19‰ to −0.11‰ of $\Delta^{199}Hg$, and −0.05‰–0.04‰ of $\Delta^{200}Hg$ (Table S4). The $\Delta^{199}Hg$ and $\delta^{202}Hg$ both show an increase trend with the increasing depth of soil profiles and the largest shift of $\delta^{202}Hg$ between moss and deepest soil is up to 1.26‰, and up to 0.08‰ for $\Delta^{199}Hg$. The more positive $\delta^{202}Hg$ and $\Delta^{199}Hg$ in soil profiles can be attributed to the Hg post-depositional processes. For example, the atmospheric Hg^0 and Hg^{II} sources mixing would lead to the both positive $\delta^{202}Hg$ and $\Delta^{199}Hg$ in soil profiles; the microbial reduction induced Hg^0 re-emission can induce more positive $\delta^{202}Hg$ in soil profiles (Kritee et al., 2008; Kritee et al., 2013; Sonke, 2011).

4. Discussion

4.1. Pathways and potential factors for heavy metals accumulation in moss

There are several roles of moss in facilitating the accumulation of heavy metals in organic soils. One is that heavy metals directly uptake by moss, then with the decomposition of moss as the organic detritus into soils. In addition, heavy metals are absorbed by the organic matters which derived from the decomposition of moss. Moreover, moss may help the moraine weathering, leading to geological sources mixing into organic soils. Finally, moss induced the lowing pH in organic soils likely results in the elevated heavy metals runoff.

Without a root and cuticle layer system lead to moss cell walls easily accessible for heavy metal ions and absorbing over the entire surface (Onianwa, 2001; Stankovic et al., 2018; Tyler, 1990). Moss accumulates heavy metals via the intracellular and extracellular processes. Briefly, the intracellular process is that heavy metals are reversible absorbed on the cell surface and then trapped as particulate matter within the surface layer or transported inside the cell; for the extracellular process, absorbed metals are bound in exchangeable form or chelating sites on the cell wall and outer surface of the plasma membrane (Onianwa, 2001; Stankovic et al.,

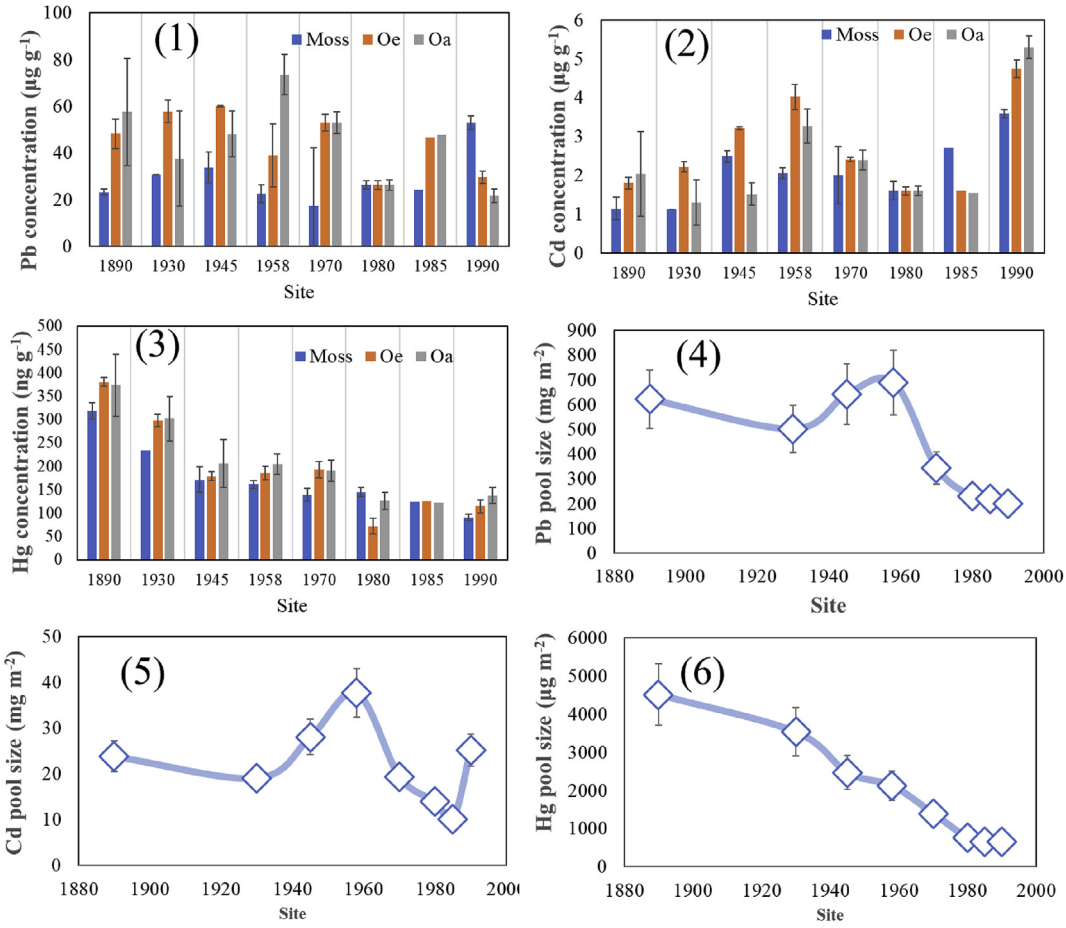

Fig. 3. (1–3) Variations of Pb, Cd and Hg concentrations in moss, Oe and Oa over the glacial erratic chronosequence; (4–6) variations of Pb, Cd and Hg pool size over the glacial erratic chronosequence.

2018; Tyler, 1990).

There are numerous sources and factors to influence heavy metal concentration in the moss. One is that the atmospheric depositions into moss surface via wet deposition, or dry deposition that later be solubilized or washed away with precipitation (Stankovic et al., 2018). In addition, though moss not like the vascular plants to directly absorb heavy metals from soil by root, the local soil still significantly contributes to the heavy metal concentration in the moss. This is because many substances in soil can be transported as the form of solutes via precipitation and runoff water to the surface of moss, or windblown particles from the ground retaining on the surface of moss (Klos et al., 2012; Salemaa et al., 2004; Stankovic et al., 2018). Besides these, the process of heavy metals leaching from the surface of vascular plants can contribute to the source in the moss on forest floor (Solberg and Selmerolsen, 1978; Stankovic et al., 2018). In this study, since quite small litterfall and throughfall input are from forest canopy due to the canopy gap over glacial erratic, the atmospheric depositions and glacier moraine particle mainly contribute to the trace elements sources in the moss.

Given Pb and Cd transport and deposition highly related to particle form, water bringing or dissolving particles on the surface of moss plays important role in facilitating their uptake processes (Bargagli, 2016; Stankovic et al., 2018). Besides Hg^{2+} uptake by moss as the patterns of Pb and Cd, atmospheric Hg^0 uptake by moss cannot be ignored. Since Hg^0 slightly soluble in water and easily re-emitting back to atmosphere, it has been suggested that once taken up, Hg^0 vapor is readily transformed into Hg^{2+}, which is nonvolatile and has a low mobility in the moss (Bargagli, 2016; Vannini et al., 2014). Furthermore, several researches suggest that moss can take up Hg^0 vapor rapidly and linearly from the atmospheric with the small Hg^0 re-emission (Bargagli, 2016; Lodenius et al., 2003; Vannini et al., 2014), and only distinct Hg mass loss when moving the moss from the contaminated site to ambient site (Lodenius et al., 2003; Lodenius, 2013). Thus, a longer atmospheric exposure time for atmospheric Hg^0 uptake likely contributes to the higher Hg concentration in moss at the earlier glacial retreated sites.

4.2. Principle component analysis

We used the principle component analysis (PCAs) to depict relations of Hg, Cd and Pb to other trace elements in moss and soils over glacier erratic. PCAs in Table 1 suggests that lithium (Li), beryllium (Be), vanadium (V), cobalt (Co), nickel (Ni), copper (Cu), gallium (Ga), arsenic (As), rubidium (Rb), strontium (Sr), molybdenum (Mo), cesium (Cs), barium (Ba), thallium (Tl) and uranium (U) have more than 0.50 factor loadings in first principle component (PC1), specifically, the factor loading $\geq$ 0.90 for Li, V, Co, Ni, Ga, Rb and Cs. We found high factor loadings of As, antimony (Sb), Hg and Pb in PC2, and high factor loadings of manganese (Mn), Cu, zinc (Zn) and Cd in PC3, and high factor loading of chromium (Cr) in PC4. Variations of pool sizes for other important trace elements, such Li, Cu, Zn, Mn, As, Cr and Sb, have been discussed in detail in SI.

It has been well documented that Li, Be, V, Co, Ni, Ga, Cs, Sr and

Table 1
Using PCAs to explain variations of trace elements in moss and soils above glacier erratic.

Variable	PCAs Component (86% of variances explained)			
	PC1 (55%)	PC2 (17%)	PC3 (10%)	PC4 (4%)
Li	**0.94**	0.06	0.21	0.14
Be	**0.89**	0.19	−0.17	0.27
V	**0.97**	0.06	0.00	0.14
Cr	0.30	−0.20	0.23	**0.83**
Mn	0.48	−0.24	**0.54**	0.16
Co	**0.90**	0.03	0.23	0.25
Ni	**0.90**	0.03	0.25	0.22
Cu	**0.56**	−0.13	**0.69**	0.18
Zn	−0.29	−0.07	**0.89**	−0.04
Ga	**0.95**	0.17	−0.09	0.14
As	0.59	**0.72**	0.00	−0.07
Rb	**0.92**	−0.07	−0.03	0.03
Sr	**0.80**	0.17	−0.01	0.46
Mo	**0.88**	−0.01	−0.10	−0.06
Cd	−0.26	0.16	**0.84**	0.16
Sb	0.17	**0.93**	−0.07	−0.15
Cs	**0.91**	0.19	−0.06	−0.17
Ba	**0.87**	0.16	−0.23	0.27
Tl	**0.73**	0.43	0.12	0.23
Pb	0.08	**0.96**	0.04	0.05
U	**0.80**	0.11	−0.20	0.27
Hg	−0.26	**0.54**	−0.39	−0.48

Note. Varimax was used as the rotation method in PCA analyses. KMO (Kaiser-Meyer-Olkin) is up to 0.842, indicating our data very suited for PCAs. Number in bold font means the significant factor loading.

Ba are mainly crust-derived in background organic soils (Tchounwou et al., 2012). Therefore, PC1 represents the crustal sources. In addition, the moraine content is dominated by silicates (~90%) at our sites, and Li content in background soils is highly related to the silicate-weathering process (Gou et al., 2017; Yang et al., 2015b). The Li concentration in rock and moraine is 6–7 times higher than in moss and soils (Table S3), suggesting the rock and moraine can be the important source over glacier erratic. Finally, the Li pool size does not exhibit a distinct increase with the increasing year after glacier retreated as Hg, Pb and Cd (Fig. S2). Hence, we selected Li as the proxy index to reflect the crustal influence, and as the reference element to calculate the EF in equation (3).

Trace elements with high factor loadings in PC2–PC4 are mainly as the heavy metals and tend to be influenced by anthropogenic activities (Tchounwou et al., 2012; Tyler, 1990). The PC2 has up to 0.96 factor loading for Pb, while 0.54 factor loading for Hg. This suggests certain similarity of Hg and Pb accumulation processes, while more important for the distinct dissimilarity between Hg and Pb. This is because different from the Pb deposition associated with aerosol physiochemistry, Hg^0 dry deposition plays an important role in Hg biogeochemical processes (Lindberg et al., 2007; Obrist et al., 2018). Lead and Cd once emitted to air, are subject to atmospheric transport with the fine particle form, and deposit into terrestrial ecosystems via dry deposition in particle form and wet deposition in precipitation. The PCAs classified Pb and Cd in different principle components (i.e., Pb in PC2 and Cd in PC3), indicating the different post-depositional processes existing between Pb and Cd over glacial erratic.

4.3. Pb and Cd sources over glacial erratic

We observed enhanced Pb during the whole chronosequence (all EF > 10), suggesting atmospheric Pb depositions play an important role. This can be further supported by several evidences. One is that the PCAs results indicate Pb biogeochemical cycling is much different from the cycling of crustal elements (e.g., Li) because of a much higher loading factor for Pb in PC2. In addition, a strong evidence from an earlier study by using Pb isotopic ratios at our glacier retreated regions clearly showed that the Pb isotope composition in the moss was comparable to in organic soils, but different from in rock and moraine (Bing et al., 2014). The further Pb mixing model suggested that anthropogenic Pb contribution was up to 42% (at 1958 site) to 66% (1890 site) in the moss, and 45% (at 1958 site) to 60% (at 1890 site) in organic soils (Bing et al., 2014). The highest crustal Pb sources around 1958 site is also supported by our data, since both Li and Pb pool sizes peak at 1958 site (The reason for Li peak discussed in detail in SI; Figs. S2 and 3), and such peak value is even higher than sizes at 1890–1930 sites, which have received much longer time atmospheric depositions.

For Cd, we observed enhanced enrichment factor in moss and soils over glacial erratic. Hence, atmospheric Cd depositions are the important sources. In addition, a higher pool size occurs around 1958 site and 1990 site as Li (The reason for Li peaks discussed in detail in SI), also suggesting the crustal Cd influences. Different from Pb, Cd has much lower retention in acid soils (Covelo et al., 2007; Majewska et al., 2007; Vega et al., 2010). It is noteworthy that the pH ranges 6.1 to 6.6 at 1990–1945 site, while decreases to 4.8 ± 0.1 at 1890 site. The substantial humus formation, some pine and spruce litters mixing (the dominant tree species as pine and spruce around 1930 and 1890 sites) and organic soil development likely contribute to such pH decrease. Lowering of pH leads to two distinct impacts. One is that reducing Cd intracellular uptake and extracellular binding, thus resulting in a lower concentration in the moss (Klos et al., 2012; Salemaa et al., 2004; Stankovic et al., 2018). The other is that the pH reduction increases the desorption of Cd in soils leading to distinct leaching with runoff (Loganathan et al., 2012; Tchounwou et al., 2012). These can be supported by that Cd concentrations at 1930–1890 sites (pH of 4.7–4.8) are about 2 times lower than at 1945 site where with pH of 6.1, and total pool sizes at 1930–1890 sites are also 15–32% lower.

4.4. Hg sources and deposition pathways

The enhanced Hg accumulation in moss and soils (40–90 times higher than the concentration in rock and moraine; EF with average value of 365 ± 278) over glacial erratic indicates the ignored crustal influences. Hence, atmospheric Hg depositions are the main sources. The atmospheric Hg depositions can be divided in two groups. One is the atmospheric Hg^0 uptake by vegetation (i.e, dry deposition of Hg^0), and the other is the Hg^{II} deposition including dry and wet depositions. Atmospheric Hg^{II} and Hg^0 depositions show distinctly different Hg isotopic compositions, especially in their MIF signatures (Biswas et al., 2008; Demers et al., 2013; Enrico et al., 2016; Jiskra et al., 2015; Wang et al., 2017; Zheng et al., 2016). Hence, we used Hg isotopic signatures to determine the contributions of atmospheric Hg^0 dry deposition and atmospheric Hg^{II} deposition over glacial erratic.

The Hg MIF signatures are much less likely to be affected by post-depositional processes than MDF in terrestrial ecosystems, making the MIF signatures as a useful tracer to identify the contribution of a specific atmospheric Hg deposition (Blum et al., 2014; Sonke, 2011; Wang et al., 2017). Earlier Hg isotope studies have well documented that the soil Hg photo-reduction and organic matter redox with Hg can induce the distinct ^{199}Hg MIF (Blum et al., 2014; Jiskra et al., 2015; Zheng et al., 2018). The positive $\Delta^{200}Hg$ signal is mainly found in precipitation, and few geochemical processes in soils can induce ^{200}Hg MIF (Chen et al., 2012; Demers et al., 2013; Gratz et al., 2010; Sherman et al., 2012; Yuan et al., 2015). Therefore, the double mixing model using $\Delta^{200}Hg$ signatures was set up to estimate atmospheric Hg^0 and Hg^{II}

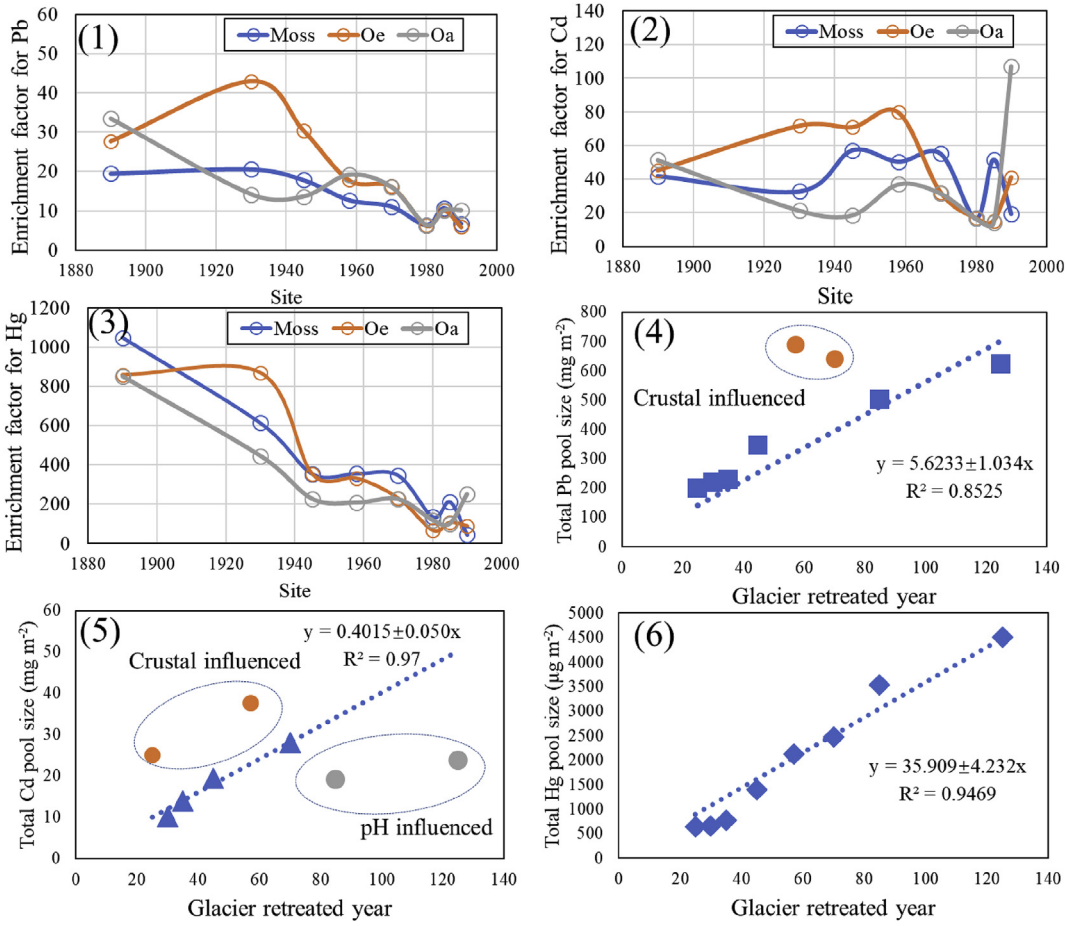

Fig. 4. Variations of enrichment factor (EF, the ratio of C/Li in moss and soils over the ratio in rock) for Pb (1), Cd (2), and Hg (3) at each site over the glacial erratic chronosequence. Estimated the average of atmospheric Pb (4), Cd (5) and Hg (6) accumulation rates over glacial erratic by using the slope of pool size versus glacier retreated time. The slope is estimated with 95% confidence bounds.

contributions in moss and soils (details in Method). We used the average value of Δ^{200}Hg in air (−0.04 ± 0.04‰) to represent the atmospheric Hg^0 endmember (Demers et al., 2013; Fu et al., 2016; Yu et al., 2016; Yuan et al., 2019) and in precipitation (0.25 ± 0.14‰) as the atmospheric Hg^{II} endmember (Chen et al., 2012; Demers et al., 2013; Gratz et al., 2010; Sherman et al., 2012; Yuan et al., 2015).

Results from the endmember mixing model show that atmospheric Hg^0 accounts for 74 ± 35% Hg in moss, and 80 ± 34% in 0–1 cm depth, and 75 ± 34% in 2–3 cm depth, 76 ± 31% in 3–5 cm depth, and 82 ± 33% in 5–7 cm depth, and 78 ± 34% in 8–9 cm depth organic soil at 1890 site. This is consistent with earlier studies that Hg in moss mainly derived from the atmospheric Hg^0 (Enrico et al., 2016; Obrist et al., 2017; Olson et al., 2019). Flux measurements highlighted the "cold trapping" inducing the elevated Hg^{II} wet position via precipitation, throughfall and cloudwater in alpine regions ecosystems (Blackwell and Driscoll, 2015; Gerson et al., 2017; Townsend et al., 2014), whereas the Hg stable isotopes in this study depict atmospheric Hg^0 uptake by moss being the primary source in organic soils over glacier erratic. This is consistent

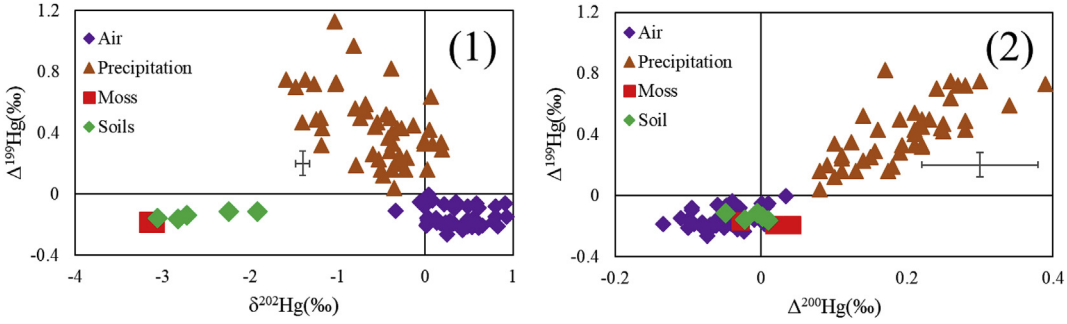

Fig. 5. Relationships among Δ^{200}Hg, δ^{202}Hg, and Δ^{199}Hg for precipitation, air, moss, 0–1 cm depth, 2–3 cm depth, 4–5 cm depth, 6–7 cm depth, and 8–9 cm depth organic soil at 1890 site. The Hg isotopic signatures in precipitation are from literatures (Chen et al., 2012; Demers et al., 2013; Gratz et al., 2010; Sherman et al., 2012; Yuan et al., 2015), and in air from literatures (Demers et al., 2013; Fu et al., 2016; Yu et al., 2016; Yuan et al., 2019).

with earlier studies that atmospheric Hg^0 uptake by vegetation dominates the organic soil Hg sources (Demers et al., 2013; Enrico et al., 2016; Jiskra et al., 2015; Wang et al., 2017; Zheng et al., 2016).

4.5. Average of Pb, Cd and Hg accumulation rates

The Pb concentration over glacial erratic is comparable to values reported in other alpine regions (Huang et al., 2008; Klaminder et al., 2005; Szopka et al., 2013; Tang et al., 2015), but ~2 times higher than the geochemical baseline value (26 $\mu g\, g^{-1}$) of China (Cheng, 2003). Given Pb pool size almost linearly increases with the glacier retreated time (except for 1945 and 1954 sites, Fig. 4), we used the slope of pool size versus glacier retreated time to estimate the average Pb accumulation rate. The average Pb accumulation rate over last 125-year is 5.6 ± 1.0 mg m^{-2} yr^{-1}. The average of atmospheric accumulation rate is usually lower than the total atmospheric deposition flux because of the output flux. The average Pb accumulation rate is about 3 times lower than the atmospheric Pb total deposition flux (14.1 mg m^{-2} yr^{-1}) at the rural site of Northern China (Pan and Wang, 2015), but 1–3 times than fluxes at rural sites of North America and Europe (Golomb et al., 1997; Kyllönen et al., 2009; Sweet et al., 1998). These suggest a potential risk of the Pb pollution at Mt. Gonnga if still elevated Pb deposition flux in future.

Except for the significant crustal influenced and pH influenced sites in Fig. 4, the average Cd accumulation rate is about 0.4 ± 0.1 mg m^{-2} yr^{-1}. From the lake and ombrotrophic peat bog sediments, Norton et al. (1990) suggested 0.1–0.2 mg m^{-2} yr^{-1} in rural/remote regions of North America. The usual Cd accumulation rate in peatlands of Europe is also less than 0.2 mg m^{-2} yr^{-1}, only several polluted sites with 0.2–0.4 mg m^{-2} yr^{-1} Cd accumulation rates (Coggins et al., 2006; Jensen, 1997; Rausch et al., 2005). From Pan and Wang (2015), the Cd atmospheric deposition ranges 0.3–0.6 mg m^{-2} yr^{-1} with the average of 0.5 ± 0.2 mg m^{-2} yr^{-1} in 10 cities of Northern China, consistent with our accumulation rate.

Over the 125-year period after glacier retreated, Hg accumulates to 4513 ± 422 $\mu g\, m^{-2}$ yr^{-1} over glacial erratic (1890 site). Such Hg pool is comparable to those found in mature temperate/boreal forest ecosystems in North America and Europe (3400–5800 $\mu g\, m^{-2}$) (Juillerat et al., 2012; Navrátil et al., 2014; Obrist et al., 2012; Richardson and Friedland, 2015), but 2–5 times lower than values in montane evergreen broadleaf forest ecosystems (Wang et al., 2016b). From Hg isotope mixing model at 1890 site, the average 78% contribution of atmospheric Hg^0 to the soil Hg pool size over glacier erratic. We assumed such average contribution can be applied to the whole glacial erratic chronosequence. This is because the atmospheric Hg^0 contributions in each depth of soil are comparable at 1890 site, though Hg in each soil horizon derived from different time atmospheric depositions. Hence, the average accumulation rate of atmospheric Hg^0 over last 125-year is 27.6 ± 3.2 $\mu g\, m^{-2}$ yr^{-1} (i.e., total Hg accumulation rate is 35.9 ± 4.2 $\mu g\, m^{-2}$ yr^{-1} in Fig. 4). Such atmospheric Hg^0 accumulation rate is larger than Amos et al. (2015) reported an average of 21.1 ± 9.1 $\mu g\, m^{-2}$ yr^{-1} present accumulation rate at 21 peatland sites, and also greater than the average value of litterfall Hg deposition (15.2 ± 8.4 $\mu g\, m^{-2}$ yr^{-1}, usually as the atmospheric Hg^0 dry deposition in forests) in global temperate/boreal forest ecosystems (Wang et al., 2016a).

The elevated accumulation rates of Pb, Cd and Hg in this study can be attributed two causes. One is that the heavy Pb, Cd and Hg atmospheric pollution in China and neighbouring regions (Fu et al., 2015; Pan and Wang, 2015). For example, Fu et al. (2010) conducted atmospheric Hg^0 measurements at Mt. Gonnga (1600 m a.s.l), about 50 km distances away from our studied sites during 2005–2007, and found that atmospheric Hg^0 concentration was about 2.8–3.2 ng m^{-3}, ~2 times higher than the background value of Northern Hemisphere (1.4–1.6 ng m^{-3}) (Sprovieri et al., 2016). The other is the intensive moss cover at Mt. Gongga, thus inducing high rate of uptake. Sun et al. (2013) reported the moss biomass at Mt. Gongga can be up to 200–600 g m^{-2}, consistent with 110–540 g m^{-2} (220 ± 140, g m^{-2}, $n = 24$) in this study (Fig. S3). Such moss biomass is almost comparable to the average litterfall biomass production (269 ± 112 g m^{-2}, $n = 99$) in temperate/boreal forest ecosystems (Wang et al., 2016a; Wang et al., 2016b). Thus, the high moss biomass is also possibly as the reason for elevated Pb, Cd and Hg accumulation rates.

5. Conclusion

This study shows that Hg, Pb and Cd are heavily enriched in a moss-dominated ecosystem over glacial erratic, and atmospheric depositions are the major sources. More in detail, atmospheric depositions via particle and precipitation dominantly contribute to the Pb sources, and followed by the moraine particles influences. The Cd variation is mainly controlled by the atmospheric depositions, and then impacts from the natural process of moraine particles and the lowering pH in soils. Atmospheric Hg^0 uptake by moss is the predominant pathway of Hg accumulation, and then the Hg wet deposition (20–25% contribution). The average Pb accumulation rate over last 125-year is about 5.6 ± 1.0 mg m^{-2} yr^{-1}, and for Cd is 0.4 ± 0.1 mg m^{-2} yr^{-1}, and for Hg^0 is 27.6 ± 3.2 $\mu g\, m^{-2}$ yr^{-1}. These elevated accumulation rates are caused by the high moss biomass and elevated atmospheric Hg, Pb and Cd pollution levels in China and neighbouring regions. In addition, we suggest further studies to investigate the Cd runoff and soil leaching, thus comprehensively assessing the Cd pollution risk in the glacial downstream aquatic ecosystems. Overall, our study indicates that the moss not only as the bioindicator, but also plays an important role in heavy metals biogeochemical cycling, specifically for Hg^0 accumulation in alpine regions. We recommend more studies on this issue in other alpine regions to systematically asses the moss role in heavy metals global biogeochemical cycling.

Acknowledgments

This research was financially supported by Natural Science Foundation of China (41703135 and 41573105), and the Strategic Priority Research Programs of the Chinese Academy of Sciences, the Pan-Third Pole Environment Study for a Green Silk Road (Pan-TPE, XDA2004050201).

Appendix A. Supplementary data

Supplementary data to this article can be found online at https://doi.org/10.1016/j.envpol.2019.112974.

References

Abrahim, G.M.S., Parker, R.J., 2008. Assessment of heavy metal enrichment factors and the degree of contamination in marine sediments from Tamaki Estuary, Auckland, New Zealand. Environ. Monit. Assess. 136, 227–238.

Amos, H.M., Sonke, J.E., Obrist, D., Robins, N., Hagan, N., Horowitz, H.M., Mason, R.P., Witt, M., Hedgecock, I.M., Corbitt, E.S., Sunderland, E.M., 2015. Observational and modeling constraints on global anthropogenic enrichment of mercury. Environ. Sci. Technol. 49, 4036–4047.

Bacardit, M., Camarero, L., 2010. Atmospherically deposited major and trace elements in the winter snowpack along a gradient of altitude in the Central Pyrenees: the seasonal record of long-range fluxes over SW Europe. Atmos. Environ. 44, 582–595.

Bargagli, R., 2016. Moss and lichen biomonitoring of atmospheric mercury: a review. Sci. Total Environ. 572, 216–231.

Bing, H.J., Wu, Y.H., Zhou, J., Li, R., Luo, J., Yu, D., 2016. Vegetation and cold trapping modulating elevation-dependent distribution of trace metals in soils of a high

mountain in eastern Tibetan plateau. Sci. Rep. 6.
Bing, H.J., Wu, Y.H., Zhou, J., Ming, L.L., Sun, S.Q., Li, X.D., 2014. Atmospheric deposition of lead in remote high mountain of eastern Tibetan Plateau, China. Atmos. Environ. 99, 425–435.
Biswas, A., Blum, J.D., Bergquist, B.A., Keeler, G.J., Xie, Z.Q., 2008. Natural mercury isotope variation in coal deposits and organic soils. Environ. Sci. Technol. 42, 8303–8309.
Blackwell, B.D., Driscoll, C.T., 2015. Using foliar and forest floor mercury concentrations to assess spatial patterns of mercury deposition. Environ. Pollut. 202, 126–134.
Blum, J.D., Bergquist, B.A., 2007. Reporting of variations in the natural isotopic composition of mercury. Anal. Bioanal. Chem. 388, 353–359.
Blum, J.D., Sherman, L.S., Johnson, M.W., 2014. Mercury isotopes in Earth and environmental Sciences. Annu. Rev. Earth Planet Sci. 42 42, 249–269.
Britton, A.J., Mitchell, R.J., Fisher, J.M., Riach, D.J., Taylor, A.F.S., 2018. Nitrogen deposition drives loss of moss cover in alpine moss-sedge heath via lowered C: N ratio and accelerated decomposition. New Phytol. 218, 470–478.
Brun, F., Berthier, E., Wagnon, P., Kaab, A., Treichler, D., 2017. A spatially resolved estimate of High Mountain Asia glacier mass balances from 2000 to 2016. Nat. Geosci. 10, 668.
Cannone, N., Gerdol, R., 2003. Vegetation as an ecological indicator of surface instability in rock glaciers. Arctic Antarct. Alpine Res. 35, 384–390.
Chen, J.B., Hintelmann, H., Feng, X.B., Dimock, B., 2012. Unusual fractionation of both odd and even mercury isotopes in precipitation from Peterborough, ON, Canada. Geochem. Cosmochim. Acta 90, 33–46.
Cheng, S., 2003. Heavy metal pollution in China: origin, pattern and control. Environ. Sci. Pollut. Control Ser. 10, 192–198.
Coggins, A.M., Jennings, S.G., Ebinghaus, R., 2006. Accumulation rates of the heavy metals lead, mercury and cadmium in ombrotrophic peatlands in the west of Ireland. Atmos. Environ. 40, 260–278.
Covelo, E.F., Vega, F.A., Andrade, M.L., 2007. Simultaneous sorption and desorption of Cd, Cr, Cu, Ni, Pb, and Zn in acid soils I. selectivity sequences. J. Hazard Mater. 147, 852–861.
Demers, J.D., Blum, J.D., Zak, D.R., 2013. Mercury isotopes in a forested ecosystem: implications for air-surface exchange dynamics and the global mercury cycle. Glob. Biogeochem. Cycles 27, 222–238.
Dyurgerov, M., 2003. Mountain and subpolar glaciers show an increase in sensitivity to climate warming and intensification of the water cycle. J. Hydrol. 282, 164–176.
Dyurgerov, M.B., Meier, M.F., 1997. Mass balance of mountain and subpolar glaciers: a new global assessment for 1961-1990. Arct. Alp. Res. 29, 379–391.
Elbert, W., Weber, B., Burrows, S., Steinkamp, J., Buedel, B., Andreae, M.O., Poeschl, U., 2012. Contribution of cryptogamic covers to the global cycles of carbon and nitrogen. Nat. Geosci. 5, 459–462.
Enrico, M., Le Roux, G., Marusczak, N., Heimburger, L.E., Claustres, A., Fu, X.W., Sun, R.Y., Sonke, J.E., 2016. Atmospheric mercury transfer to peat bogs dominated by gaseous elemental mercury dry deposition. Environ. Sci. Technol. 50, 2405–2412.
Estrade, N., Carignan, J., Sonke, J.E., Donard, O.F.X., 2010. Measuring Hg isotopes in bio-geo-environmental reference materials. Geostand. Geoanal. Res. 34, 79–93.
Favero-Longo, S.E., Worland, M.R., Convey, P., Lewis Smith, R.I., Piervittori, R., Guglielmin, M., Cannone, N., 2012. Primary succession of lichen and bryophyte communities following glacial recession on signy island, south orkney islands, maritime antarctic. Antarct. Sci. 24, 323–336.
Frenot, Y., Gloaguen, J.C., Cannavacciuolo, M., Bellido, A., 1998. Primary succession on glacier forelands in the subantarctic Kerguelen Islands. J. Veg. Sci. 9, 75–84.
Fu, X., Zhu, W., Zhang, H., Sommar, J., Yu, B., Yang, X., Wang, X., Lin, C.-J., Feng, X., 2016. Depletion of atmospheric gaseous elemental mercury by plant uptake at Mt. Changbai, Northeast China. Atmos. Chem. Phys. 16, 12861–12873.
Fu, X.W., Feng, X.B., Zhu, W.Z., Rothenberg, S., Yao, H., Zhang, H., 2010. Elevated atmospheric deposition and dynamics of mercury in a remote upland forest of southwestern China. Environ. Pollut. 158, 2324–2333.
Fu, X.W., Zhang, H., Yu, B., Wang, X., Lin, C.J., Feng, X.B., 2015. Observations of atmospheric mercury in China: a critical review. Atmos. Chem. Phys. 15, 9455–9476.
Gerson, J.R., Driscoll, C.T., Demers, J.D., Sauer, A.K., Blackwell, B.D., Montesdeoca, M.R., Shanley, J.B., Ross, D.S., 2017. Deposition of mercury in forests across a montane elevation gradient: elevational and seasonal patterns in methylmercury inputs and production. Journal of Geophysical Research-Biogeosciences 122, 1922–1939.
Golomb, D., Ryan, D., Eby, N., Underhill, J., Zemba, S., 1997. Atmospheric deposition of toxics onto Massachusetts Bay—I. Metals. Atmos. Environ. 31, 1349–1359.
Gou, L.-F., Jin, Z.D., He, M., 2017. Using Lithium Isotopes Traces Continental Weathering: Progresses and Challenges.
Gratz, L.E., Keeler, G.J., Blum, J.D., Sherman, L.S., 2010. Isotopic composition and fractionation of mercury in great lakes precipitation and ambient air. Environ. Sci. Technol. 44, 7764–7770.
Huang, J.-H., Kalbitz, K., Matzner, E., 2008. Mobility of trimethyllead and total lead in the forest floor. Soil Sci. Soc. Am. J. 72, 978–984.
Jensen, A., 1997. Historical deposition rates of Cd, Cu, Pb, and Zn in Norway and Sweden estimated by210Pb dating and measurement of trace elements in cores of peat bogs. Water Air Soil Pollut. 95, 205–220.
Jiskra, M., Wiederhold, J.G., Skyllberg, U., Kronberg, R.M., Hajdas, I., Kretzschmar, R., 2015. Mercury deposition and Re-emission pathways in boreal forest soils investigated with Hg isotope signatures. Environ. Sci. Technol. 49, 7188–7196.
Juillerat, J.I., Ross, D.S., Bank, M.S., 2012. Mercury in litterfall and upper soil horizons in forested ecosystems in Vermont, USA. Environ. Toxicol. Chem. 31, 1720–1729.
Klaminder, J., Bindler, R., Emteryd, O., Renberg, I., 2005. Uptake and recycling of lead by boreal forest plants: quantitative estimates from a site in northern Sweden. Geochem. Cosmochim. Acta 69, 2485–2496.
Klos, A., Rajfur, M., Sramek, I., Waclawek, M., 2012. Mercury concentration in lichen, moss and soil samples collected from the forest areas of Praded and Glacensis Euroregions (Poland and Czech Republic). Environ. Monit. Assess. 184, 6765–6774.
Kritee, K., Blum, J.D., Barkay, T., 2008. Mercury stable isotope fractionation during reduction of Hg(II) by different microbial pathways. Environ. Sci. Technol. 42, 9171–9177.
Kritee, K., Blum, J.D., Reinfelder, J.R., Barkay, T., 2013. Microbial stable isotope fractionation of mercury: a synthesis of present understanding and future directions. Chem. Geol. 336, 13–25.
Kyllönen, K., Karlsson, V., Ruoho-Airola, T., 2009. Trace element deposition and trends during a ten year period in Finland. Sci. Total Environ. 407, 2260–2269.
Lindberg, S., Bullock, R., Ebinghaus, R., Engstrom, D., Feng, X.B., Fitzgerald, W., Pirrone, N., Prestbo, E., Seigneur, C., 2007. A synthesis of progress and uncertainties in attributing the sources of mercury in deposition. Ambio 36, 19–32.
Lodenius, A., Tulisalo, E., Soltanpour-Gargari, A., 2003. Exchange of mercury between atmosphere and vegetation under contaminated conditions. Sci. Total Environ. 304, 169–174.
Lodenius, M., 2013. Use of plants for biomonitoring of airborne mercury in contaminated areas. Environ. Res. 125, 113–123.
Loganathan, P., Vigneswaran, S., Kandasamy, J., Naidu, R., 2012. Cadmium sorption and desorption in soils: a review. Crit. Rev. Environ. Sci. Technol. 42, 489–533.
Luo, J., Li, W., She, J., He, Y., Gao, J., 2017. Carbon dynamics in different primary succession stages on Hailuogou Glacier forehead in mount Gongga,China. Mt. Res. 35, 629–635.
Majewska, M., Kurek, E., Rogalski, J., 2007. Microbially mediated cadmium sorption/desorption processes in soil amended with sewage sludge. Chemosphere 67, 724–730.
Miguez, F., Fernandez-Marin, B., Becerril, J.M., Garcia-Plazaola, J.I., 2017. Diversity of winter photoinhibitory responses: a case study in co-occurring lichens, mosses, herbs and woody plants from subalpine environments. Physiol. Plant. 160, 282–296.
Nakatsubo, T., Uchida, M., Sasaki, A., Kondo, M., Yoshitake, S., Kanda, H., 2015. Carbon accumulation rate of peatland in the High Arctic, Svalbard: implications for carbon sequestration. Polar Science 9, 267–275.
Navrátil, T., Shanley, J., Rohovec, J., Hojdová, M., Penížek, V., Buchtová, J., 2014. Distribution and pools of mercury in Czech forest soils. Water, Air & Soil Pollution 225, 1829.
Norton, S.A., Dillon, P.J., Evans, R.D., Mierle, G., Kahl, J.S., 1990. The history of atmospheric deposition of Cd, Hg, and Pb in North America: evidence from lake and peat bog sediments. In: Lindberg, S.E., Page, A.L., Norton, S.A. (Eds.), Acidic Precipitation: Sources, Deposition, and Canopy Interactions. Springer New York, New York, NY, pp. 73–102.
Obrist, D., Agnan, Y., Jiskra, M., Olson, C.L., Colegrove, D.P., Hueber, J., Moore, C.W., Sonke, J.E., Helmig, D., 2017. Tundra uptake of atmospheric elemental mercury drives Arctic mercury pollution. Nature 547, 201–204.
Obrist, D., Johnson, D.W., Edmonds, R.L., 2012. Effects of vegetation type on mercury concentrations and pools in two adjacent coniferous and deciduous forests. J. Plant Nutr. Soil Sci. 175, 68–77.
Obrist, D., Kirk, J.L., Zhang, L., Sunderland, E.M., Jiskra, M., Selin, N.E., 2018. A review of global environmental mercury processes in response to human and natural perturbations: changes of emissions, climate, and land use. Ambio 47, 116–140.
Olson, C.L., Jiskra, M., Sonke, J.E., Obrist, D., 2019. Mercury in tundra vegetation of Alaska: spatial and temporal dynamics and stable isotope patterns. Sci. Total Environ. 660, 1502–1512.
Onianwa, P.C., 2001. Monitoring atmospheric metal pollution: a review of the use of mosses as indicators. Environ. Monit. Assess. 71, 13–50.
Pan, Y.P., Wang, Y.S., 2015. Atmospheric wet and dry deposition of trace elements at 10 sites in Northern China. Atmos. Chem. Phys. 15, 951–972.
Raffl, C., Mallaun, M., Mayer, R., Erschbamer, B., 2006. Vegetation succession pattern and diversity changes in a glacier valley, central alps, Austria. Arctic Antarct. Alpine Res. 38, 421–428.
Rausch, N., Nieminen, T., Ukonmaanaho, L., Le Roux, G., Krachler, M., Cheburkin, A.K., Bonani, G., Shotyk, W., 2005. Comparison of atmospheric deposition of copper, nickel, cobalt, zinc, and cadmium recorded by Finnish peat cores with monitoring data and emission records. Environ. Sci. Technol. 39, 5989–5998.
Richardson, J.B., Friedland, A.J., 2015. Mercury in coniferous and deciduous upland forests in northern New England, USA: implications of climate change. Biogeosciences 12, 6737–6749.
Salemaa, M., Derome, J., Helmisaari, H.S., Nieminen, T., Vanha-Majamaa, I., 2004. Element accumulation in boreal bryophytes, lichens and vascular plants exposed to heavy metal and sulfur deposition in Finland. Sci. Total Environ. 324, 141–160.
Sherman, L.S., Blum, J.D., Keeler, G.J., Demers, J.D., Dvonch, J.T., 2012. Investigation of local mercury deposition from a coal-fired power plant using mercury isotopes. Environ. Sci. Technol. 46, 382–390.
Solberg, Y., Selmerolsen, A.R., 1978. Studies on chemistry of lichens and mosses .17. mercury content of several lichen and moss species collected in Norway.

Bryologist 81, 144–149.
Sonke, J.E., 2011. A global model of mass independent mercury stable isotope fractionation. Geochem. Cosmochim. Acta 75, 4577–4590.
Sprovieri, F., Pirrone, N., Bencardino, M., D'Amore, F., Carbone, F., Cinnirella, S., Mannarino, V., Landis, M., Ebinghaus, R., Weigelt, A., Brunke, E.G., Labuschagne, C., Martin, L., Munthe, J., Wängberg, I., Artaxo, P., Morais, F., Barbosa, H.D.M.J., Brito, J., Cairns, W., Barbante, C., Diéguez, M.D.C., Garcia, P.E., Dommergue, A., Angot, H., Magand, O., Skov, H., Horvat, M., Kotnik, J., Read, K.A., Neves, L.M., Gawlik, B.M., Sena, F., Mashyanov, N., Obolkin, V., Wip, D., Feng, X.B., Zhang, H., Fu, X., Ramachandran, R., Cossa, D., Knoery, J., Marusczak, N., Nerentorp, M., Norstrom, C., 2016. Atmospheric mercury concentrations observed at ground-based monitoring sites globally distributed in the framework of the GMOS network. Atmos. Chem. Phys. 16, 11915–11935.
Stankovic, J.D., Sabovljevic, A.D., Sabovljevic, M.S., 2018. Bryophytes and heavy metals: a review. Acta Bot. Croat. 77, 109–118.
Sun, S.-Q., Wu, Y.-H., Wang, G.-X., Zhou, J., Yu, D., Bing, H.-J., Luo, J., 2013. Bryophyte species richness and composition along an altitudinal gradient in Gongga mountain, China. PLoS One 8, e58131.
Sweet, C.W., Weiss, A., Vermette, S.J., 1998. Atmospheric deposition of trace metals at three sites near the great lakes. Water Air Soil Pollut. 103, 423–439.
Szopka, K., Karczewska, A., Jezierski, P., Kabała, C., 2013. Spatial distribution of lead in the surface layers of mountain forest soils, an example from the Karkonosze National Park, Poland. Geoderma 192, 259–268.
Tang, R., Luo, J., She, J., Chen, Y., Yang, D., Zhou, J., 2015. The cadmium and lead of soil in timberline coniferous forests, Eastern Tibetan Plateau. Environmental Earth Sciences 73, 303–310.
Tchounwou, P.B., Yedjou, C.G., Patlolla, A.K., Sutton, D.J., 2012. Heavy metal toxicity and the environment. Exp. Suppl. 2012 (101), 133–164.
Tóth, G., Hermann, T., Szatmári, G., Pásztor, L., 2016. Maps of heavy metals in the soils of the European Union and proposed priority areas for detailed assessment. Sci. Total Environ. 565, 1054–1062.
Townsend, J.M., Driscoll, C.T., Rimmer, C.C., McFarland, K.P., 2014. Avian, salamander, and forest floor mercury concentrations increase with elevation in a terrestrial ecosystem. Environ. Toxicol. Chem. 33, 208–215.
Tyler, G., 1990. Bryophytes and heavy-metals - a literature-review. Bot. J. Linn. Soc. 104, 231–253.
Vannini, A., Nicolardi, V., Bargagli, R., Loppi, S., 2014. Estimating atmospheric mercury concentrations with lichens. Environ. Sci. Technol. 48, 8754–8759.
Vega, F.A., Andrade, M.L., Covelo, E.F., 2010. Influence of soil properties on the sorption and retention of cadmium, copper and lead, separately and together, by 20 soil horizons: comparison of linear regression and tree regression analyses. J. Hazard Mater. 174, 522–533.
Wang, X., Bao, Z., Lin, C.-J., Yuan, W., Feng, X., 2016a. Assessment of global mercury deposition through litterfall. Environ. Sci. Technol. 50, 8548–8557.
Wang, X., Lin, C.J., Lu, Z.Y., Zhang, H., Zhang, Y.P., Feng, X.B., 2016b. Enhanced accumulation and storage of mercury on subtropical evergreen forest floor: implications on mercury budget in global forest ecosystems. Journal of Geophysical Research-Biogeosciences 121, 2096–2109.
Wang, X., Luo, J., Yin, R., Yuan, W., Lin, C.-J., Sommar, J., Feng, X., Wang, H., Lin, C., 2017. Using mercury isotopes to understand mercury accumulation in the montane forest floor of the eastern Tibetan plateau. Environ. Sci. Technol. 51, 801–809.
Wang, X., Yuan, W., Lu, Z.Y., Lin, C.J., Yin, R.S., Li, F., Feng, X.B., 2019. Effects of precipitation on mercury accumulation on subtropical montane forest floor: implications on climate forcing. Journal of Geophysical Research-Biogeosciences 124, 959–972.
Yang, D., Luo, J., She, J., Tang, R., 2015a. Dynamics of vegetation biomass along the chronosequence in Hailuogou Glacier retreated area, Mt. Gongga. Ecology and Environmental Sciences 24, 1843–1850.
Yang, Z., Bing, H., Zhou, J., Wu, Y., Sun, H., Luo, J., Sun, S., Wang, J., 2015b. Variation of mineral composition along the soil chronosequence at the hailuogou glacier foreland of Gongga mountain. Acta Pedol. Sin. 52, 507–516.
Yao, T.D., Thompson, L., Yang, W., Yu, W.S., Gao, Y., Guo, X.J., Yang, X.X., Duan, K.Q., Zhao, H.B., Xu, B.Q., Pu, J.C., Lu, A.X., Xiang, Y., Kattel, D.B., Joswiak, D., 2012. Different glacier status with atmospheric circulations in Tibetan Plateau and surroundings. Nat. Clim. Chang. 2, 663–667.
Yu, B., Fu, X., Yin, R., Zhang, H., Wang, X., Lin, C.-J., Wu, C., Zhang, Y., He, N., Fu, P., 2016. Isotopic composition of atmospheric mercury in China: new evidence for sources and transformation processes in air and in vegetation. Environ. Sci. Technol. 50, 9262–9269.
Yuan, S., Zhang, Y., Chen, J., Kang, S., Zhang, J., Feng, X., Cai, H., Wang, Z., Wang, Z., Huang, Q., 2015. Large variation of mercury isotope composition during a single precipitation event at Lhasa City, Tibetan Plateau, China. In: Millot, R., Negrel, P. (Eds.), 11th Applied Isotope Geochemistry Conference Aig-11, pp. 282–286.
Yuan, W., Sommar, J., Lin, C.-J., Wang, X., Li, K., Liu, Y., Zhang, H., Lu, Z., Wu, C., Feng, X., 2019. Stable isotope evidence shows Re-emission of elemental mercury vapor occurring after reductive loss from foliage. Environ. Sci. Technol. 53, 651–660.
Zhang, H., Yin, R.S., Feng, X.B., Sommar, J., Anderson, C.W.N., Sapkota, A., Fu, X.W., Larssen, T., 2013. Atmospheric mercury inputs in montane soils increase with elevation: evidence from mercury isotope signatures. Sci. Rep. 3, 3322.
Zheng, W., Demers, J.D., Lu, X., Bergquist, B.A., Anbar, A.D., Blum, J.D., Gu, B., 2018. Mercury Stable Isotope Fractionation during Abiotic Dark Oxidation in the Presence of Thiols and Natural Organic Matter. Environmental Science & Technology.
Zheng, W., Obrist, D., Weis, D., Bergquist, B.A., 2016. Mercury isotope compositions across North American forests. Glob. Biogeochem. Cycles 30, 1475–1492.
Zhou, J., Wu, Y., Prietzel, J., Bing, H., Dong, Y., Sun, S., Ji, L., Sun, H., 2013. Changes of soil phosphorus speciation along a 120-year soil chronosequence in the Hailuogou Glacier retreat area (Gongga Mountain, SW China). Geoderma 195, 251–259.